The American Journal of Pathology, Vol. 184, No. 3, March 2014

ELSEVIER

The American Journal of
PATHOLOGY
ajp.amjpathol.org

GASTROINTESTINAL, HEPATOBILIARY, AND PANCREATIC PATHOLOGY

Nestin Delineates Pancreatic Cancer Stem Cells in Metastatic Foci of NOD/Shi-scid IL2Rγ^{null} (NOG) Mice

Yoko Matsuda,* Hisashi Yoshimura,* Junji Ueda,*† Zenya Naito,* Murray Korc,‡ and Toshiyuki Ishiwata*

From the Departments of Pathology and Integrative Oncological Pathology, and the Department of Surgery for Organ and Biological Regulation,† Graduate School of Medicine, Nippon Medical School, Tokyo, Japan; and the Departments of Medicine and Biochemistry and Molecular Biology,‡ Indiana University School of Medicine and the Melvin and Bren Simon Cancer Center, Indianapolis, Indiana*

Accepted for publication November 18, 2013.

Address correspondence to Toshiyuki Ishiwata, M.D., Ph.D., Director of Molecular Pathology Group, Departments of Pathology and Integrative Oncological Pathology, Nippon Medical School, 1-1-5 Sendagi, Bunkyo-ku, Tokyo 113-8602, Japan. E-mail: ishiwata@nms.ac.jp.

Pancreatic ductal adenocarcinoma (PDAC) is associated with a high incidence of hepatic metastases, as well as occasional pulmonary metastases. To delineate the potential role of cancer stem cells (CSCs) in PDAC metastasis, human PDAC cells were injected into the spleen of mice. The characteristics and expression of markers associated with CSC and epithelial–mesenchymal transition (EMT) of metastatic cells that developed in the liver and lung were then compared with parental cells. The metastatic cells were polygonal, and larger than parental cells. Metastatic cells also exhibited decreased proliferation and increased adhesion to extracellular matrices, as well as enhanced migration and invasion *in vitro* and increased metastatic capacity *in vivo*. The CSC markers ALDH1A1, ABCG2, and nestin were expressed at high levels in metastatic cells and exhibited changes consistent with EMT (eg, decreased E-cadherin expression). Moreover, metastatic cells readily formed spheres in culture and exhibited an increased side population by flow analysis. Nestin and ABCG2 were also expressed at high levels in metastatic lesions from PDAC patients, and silencing nestin with shRNA in PDAC cells derived from lung metastases resulted in a marked decrease in the capacity of the cells to form spheres and to yield pulmonary or hepatic metastases. Thus, the metastatic potential of human PDAC cells correlates with CSCs and with EMT characteristics and is dependent on nestin expression. *(Am J Pathol 2014, 184: 674–685; http://dx.doi.org/10.1016/j.ajpath.2013.11.014)*

Pancreatic ductal adenocarcinoma (PDAC) is an aggressive malignancy with a high incidence of distant metastasis.[1] The metastatic process involves a series of complex biological processes, including migration, invasion, adhesion, and survival.[2] Furthermore, the extracellular matrix, interstitial cells, blood and lymph vessels, nerve fibers, and immune cells contribute to these processes. It is difficult to completely resolve the pathways that promote invasion and metastasis of PDAC cells, but elucidating the mechanisms that contribute to their enhanced metastatic efficiency is important for development of novel therapeutic approaches. Accordingly, a variety of mouse models, ranging from orthotopic models to genetically engineered mice, have been developed to study the metastatic processes that govern PDAC metastasis.

Injection of human PDAC cells into the spleen of nude mice or NOD/SCID mice is a model that yields a small number of metastatic nodules in the liver.[3] By contrast, in the recently developed NOD/Shi-scid IL2Rγ^{null} (NOG) mice (which have severe immunodeficiency, including defects in T, B, natural killer, and dendritic cell function) human pancreatic and colorectal cancer cells easily proliferate and metastasize to the liver after intrasplenic injection.[4] It is not known, however, whether cancer stem cells (CSCs) have a role in the enhanced metastatic propensity of NOG mice. CSCs exhibit pluripotency, have the potential to self-renew, and are crucially important in cancer cell growth, invasion, metastasis, and recurrence.[5–7] CSCs preferentially spread to distant organs and contribute to the formation of lesions that phenocopy the primary tumor.[8]

Given these observations, it has been suggested that targeting CSCs could provide a new therapeutic strategy in cancer.[9] It is therefore important to examine the temporal and spatial alterations of CSCs in metastatic lesions *in vivo*.

Supported in part by the Japan Society for the Promotion of Science grant-in-aid 25462127 and 25461027 (Y.M. and T.I.), the Pancreas Research Foundation of Japan (H.Y.), and NIH grant R37-CA-075059 (M.K.).

Disclosures: None declared.

http://dx.doi.org/10.1016/j.ajpath.2013.11.014

Furthermore, epithelial−mesenchymal transition (EMT), a fundamental mechanism controlling multiple events during metastasis,[10] may generate additional CSCs endowed with a more invasive, migratory, and metastatic phenotype.[11] We reasoned that NOG mice would be useful for assessing the role of CSCs in the metastatic process in PDAC, because this model avoids the complexity engendered by an active immune system.

In the present study, we analyzed pathological features of metastatic tumors originating from human PDAC cells. Metastatic PDAC cells exhibited lower growth rates, but higher migration and metastatic abilities. The metastatic lesions contained more CSCs than did primary tumors, and these cells exhibited a mesenchymal phenotype. Moreover, inhibition of one of the CSC markers, nestin, in metastatic PDAC cells reduced sphere formation *in vitro* and metastasis *in vivo*.

Materials and Methods

Materials

Antibodies were purchased as follows: mouse monoclonal anti−cytokeratin 19 (CK-19) antibody from Boehringer Mannheim Biochemical (Roche Applied Science, Mannheim, Germany); mouse monoclonal anti−human leukocyte antigen (HLA) class I-A, B, and C antibody from Hokudo (Sapporo, Japan); mouse monoclonal anti−E-cadherin, mouse monoclonal anti-vimentin, mouse monoclonal anti−Ki-67, and mouse monoclonal anti-CD68 antibodies from Dako (Kyoto, Japan; Carpinteria, CA); mouse monoclonal anti-ABCG2, rabbit polyclonal anti-ALDH1A1, mouse monoclonal anti-CD3, mouse monoclonal anti-CD11c, rabbit polyclonal anti−c-Met, and rabbit polyclonal anti-CXCR4 antibodies from Abcam (Cambridge, UK); mouse monoclonal anti-CD44 and mouse monoclonal anti-nestin antibodies from R&D Systems (Minneapolis, MN); mouse monoclonal anti-CD133, goat polyclonal anti-nestin, mouse monoclonal anti-GAPDH, and mouse monoclonal anti-CD20 antibodies from Santa Cruz Biotechnology (Santa Cruz, CA); and rat monoclonal anti−MAC-2 antibody from Cedarlane Laboratories (Burlington, ON, Canada). Matrigel invasion chambers were purchased from BD Biosciences (San Jose, CA), and various chemicals and reagents from Sigma-Aldrich (St. Louis, MO).

Human PDAC Cell Lines

Twelve human PDAC cell lines were obtained from the Cell Resource Center for Biomedical Research, Institute of Development, Aging and Cancer, Tohoku University (Sendai, Japan; ACBR-1, AsPC-1, KLM-1, MIAPaCa-2, PANC-1, PK-1, PK-45H, PK-45P, PK-59, PK-8, and PK-9) and from the ATCC (Manassas, VA; Capan-1). Cells were cultured in RPMI 1640 medium containing 10% fetal bovine serum (15% for Capan-1 cells). The PANC-1, PK-45H, and KLM-1 cell lines were authenticated by short tandem repeat profiling analysis (March 2012; data not shown).

Intrasplenic, Intrapancreatic, and Intravenous Tumor Models

PANC-1 or PK-45H cells (1×10^5 cells) were injected into the spleen of 6-week-old male NOG mice ($n = 12$ per cell line) (Central Institute for Experimental Animals, Kanagawa, Japan) and BALB/cA Jcl-*nu*/*nu* nude mice ($n = 12$ per cell line) (CLEA Japan, Tokyo, Japan). The spleen was resected 1 minute later. After 1 day and after 2, 4, and 8 weeks, three mice per time point were euthanized, and the liver, pancreas, lungs, heart, brain, and kidneys were excised.

Orthotopic implantations were performed by injecting 1×10^5 cells into the tail portion of the pancreas of NOG mice ($n = 3$ mice per cell line), which were sacrificed 8 weeks later. Tail-vein injections (1×10^5 cells) were performed in NOG mice ($n = 6$ mice per cell line), which were sacrificed 8 weeks later. All animal experiments were conducted according to the institutional animal care guidelines of the Nippon Medical School Animal Ethical Committee.

Immunohistochemistry

Paraffin-embedded sections were subjected to immunostaining using a Histofine Simple Stain MAX PO kit (Nichirei Biosciences, Tokyo, Japan). For aldehyde dehydrogenase 1 family member A1 (ALDH1A1), E-cadherin, vimentin, ATP-binding cassette subfamily G member 2 (ABCG2), CD44, CD133, Ki-67, CD3, CD20, and CD11c, tissue sections were preheated in 10 mmol/L of citrate buffer (pH 6.0). For MAC-2, tissue sections were treated in 0.1% protease for 10 minutes. Tissue sections were incubated overnight with the following antibodies and dilutions: anti-ALDH1A1 (1:100), anti−CK-19 (1:100), anti-HLA (1:100), anti−E-cadherin (1:100), anti-vimentin (1:500), anti-ABCG2 (1:100), anti-CD44 (1:10,000), anti-CD133 (1:1500), mouse monoclonal anti-nestin (1:200), anti−Ki-67 (1:100), anti-CD3 (1:400), anti-CD20 (1:800), anti−MAC-2 (1:200), anti-CD68 (1:50), and anti-CD11c (1:100). Negative controls were prepared by omitting the primary antibody. For analysis of the immunostaining results, we captured five images in each specimen at $\times 200$ magnification and then measured the areas of positive cells using WinROOF image analysis software version 6.1.3 (Mitani, Tokyo, Japan). We determined the percentage of HLA^+ cancer area as described previously,[9] and then determined the ratios of positive immunostaining for ALDH1A1, ABCG2, CD44, nestin, Ki-67, E-cadherin, and vimentin to HLA^+ cancer cell area in metastatic foci.

Detection of Human-Specific or Mouse-Specific Mitochondrial Genes

We performed PCR with human-specific and mouse-specific mitochondrial primers and a TaKaRa Ex Taq kit, Hot Start version (Takara Bio, Otsu, Japan). The human forward and reverse primers were, respectively, 5′-TATTGCAGCCCTAGCAGCACTCCA-3′ (15,311 to 15,334)

and 5′-AGAATGAGGAGGTCTGCGGC-3′ [15,732 to 15,751, 441 bp; NC_001807. (This reference sequence was removed from Genbank and replaced with record NC_012920 as the accepted reference sequence for *Homo sapiens* mitochondrion; there is only a single nucleotide difference in the forward primer and the currently recognized reference sequence.)]. The mouse forward and reverse primers were, respectively, 5′-GCACTGAAAATGCTTAGATGGATAA-TT-G-3′ (28 to 55) and 5′-CCTCTC-ATAAACGGATGTC-TA-G-3′ (954 to 975, 948 bp; NC_005089).[12]

Establishment of PDAC Cells from Metastatic Tumors

NOG mice were given a single intrasplenic injection of 1×10^5 PANC-1 or PK-45H cells. Eight weeks later, the mice were euthanized and the liver and lungs were removed. Metastatic foci were cut into 1-mm^3 cubes, and tumor fragments dispersed in a medium containing antibiotics (400 U/mL penicillin and 400 μg/mL kanamycin). Metastatic PANC-1 or PK-45H cells from liver or lung (referred to here as PANC-liver, PANC-lung, PK-liver, and PK-lung cells) were confirmed as being of human origin, using human- or mouse-specific mitochondrial gene primers as described above.

Cell Growth Assays

Cell growth was monitored with a nonradioactive proliferation assay using a WST-8 cell-counting kit (Dojindo Molecular Technologies, Kumamoto, Japan; Rockville, MD). Experiments were performed in triplicate.

Cell Adhesion, Migration, and Invasion Assays

Cell adhesion to extracellular matrices (bovine type I collagen, human type IV collagen, bovine fibronectin, and murine laminin) was determined as described previously.[9] Single-cell movement was analyzed using time-lapse microscopy, as described previously.[13] Invasion assays were performed using a modified Boyden chamber technique with Matrigel-coated inserts.[9] Experiments were performed in triplicate.

RT-qPCR

Quantitative RT-PCR (RT-qPCR) was performed using TaqMan Fast Universal PCR master mix and TaqMan gene expression assays (Life Technologies, Carlsbad, CA) for ALDH1A1 (Hs00946916_m1), E-cadherin (Hs01013953_m1), vimentin (Hs00185584_m1), ABCG2 (Hs01053790_m1), CD44 (Hs00153304_m1), CD133 (Hs01009238_m1), nestin (Hs00707120_s1), c-Met (alias hepatocyte growth factor receptor) (Hs01565584_m1), hepatocyte growth factor (HGF) (Hs00300159_m1), and 18S rRNA (Hs99999901_s1). RT-qPCR results were expressed as the ratio of target to 18S rRNA. Gene expression measurements were performed in triplicate.

Western Blot Analysis

Proteins were subjected to SDS-PAGE under nonreducing conditions. Membranes were incubated with goat polyclonal anti-nestin antibody (1:1000) and then with donkey anti-goat IgG (1:4000). Membranes were reblotted with anti-GAPDH antibody (1:5000).

Sphere-Formation Assay

Cells (1×10^3/well) were plated in a 24-well plate with an ultralow-attachment surface and supplemented with basic fibroblast growth factor (bFGF; 10 ng/mL) and pro-epidermal growth factor (EGF; 20 ng/mL).[14] After 5 days, the number of spheres was counted using phase-contrast microscopy. Experiments were performed in triplicate.

Flow Cytometry

Cells were stained with Hoechst dye 33342 (5 μg) to identify the side-population cells.[13] Verapamil (30 μg/mL) was used to verify specificity of the side-population population.

Monoclonal mouse IgG1 anti-nestin antibody was labeled with Alexa Fluor 488 using a Zenon antibody labeling kit (Life Technologies). Antibodies for ALDH1A1 (rabbit), ABCG2 (mouse IgG2a), CD44 (mouse IgG2a), CD133 (mouse), c-Met (rabbit), and CXCR4 (rabbit) were labeled with allophycocyanin. Cells were incubated for 20 minutes at 4°C in 10% human serum, and then incubated (5×10^5 cells/50 μL) with each antibody for 30 minutes at room temperature. Dead cells were labeled with the addition of 1 μg propidium iodide. We prepared rabbit IgG isotype control-treated cells as negative controls. Expression of each protein was analyzed using a BD FACSAria II flow cytometer (BD Biosciences). Experiments were performed in triplicate.

Human PDAC Autopsy Cases

Tissue sections from 12 autopsy cases (4 male, 8 female) with PDAC at Nippon Medical School Hospital (Tokyo, Japan) from 1995 to 2010 were obtained for this study. Median age was 73.9 years (range, 58 to 88 years). All 12 patients had liver metastases, 8 had lung metastases, 11 had lymph node metastases, and 9 had omental metastases. The study was conducted in accordance with the principles embodied in the 2008 Declaration of Helsinki. Only tissues that exhibited histological integrity were used for immunostaining.

Generation of Nestin shRNA-Expressing Transfectants

Nestin shRNA expression vector and sham vector[9] were transfected into PANC-liver and PANC-lung cells using FuGENE HD transfection reagent (Roche Diagnostics, Indianapolis, IN). Independent colonies were isolated by ring cloning. shRNA transfection efficiency was confirmed by RT-qPCR and Western blotting.

Statistical Analysis

Data were compared by one-way analysis of variance and χ^2 test using the StatView J software package version 5.0 (SAS Institute, Cary, NC). $P < 0.05$ was considered statistically significant.

Results

Formation of Metastatic PDAC Tumors in Immunodeficient Mice

PANC-1 and PK-45H human PDAC cells were injected into the spleen of NOG mice. Macroscopically, PANC-1 cells yielded small, white hepatic nodules at 4 weeks, and the liver was mostly replaced by metastatic tumors at 8 weeks (Figure 1A). Similar results were observed with PK-45H cells (data not shown). In addition, nondescript red nodules were detected in lung of NOG mice at 8 weeks with both PANC-1 (Figure 1A) and PK-45H (data not shown) cells. There were no macroscopic metastases in other organs and no other significant changes.

Microscopic analysis revealed the presence of metastatic cancer cells in liver of NOG mice at 8 weeks after intrasplenic injection of PANC-1 or PK-45H cells (Supplemental Figure S1A). IHC analysis using anti−CK-19 and anti-HLA revealed that PANC-1 cells metastasized to liver, lung, pancreas, kidney, and heart (Supplemental Figure S1, B−G), whereas PK-45H cells metastasized only to lung and pancreas (data not shown). In the liver, PANC-1 cells formed alveolar structures, and PK-45H cells formed gland-like structures (Supplemental Figure S1H). The extent of hepatic and lung metastases increased over time (Figure 1B), with HLA^+ cells detectable in liver of all NOG mice on days 1 through 56 after intrasplenic injection (Supplemental Table S1).

To confirm the presence of PANC-1 cells in NOG mice, PCR for human- and mouse-specific mtDNA was performed

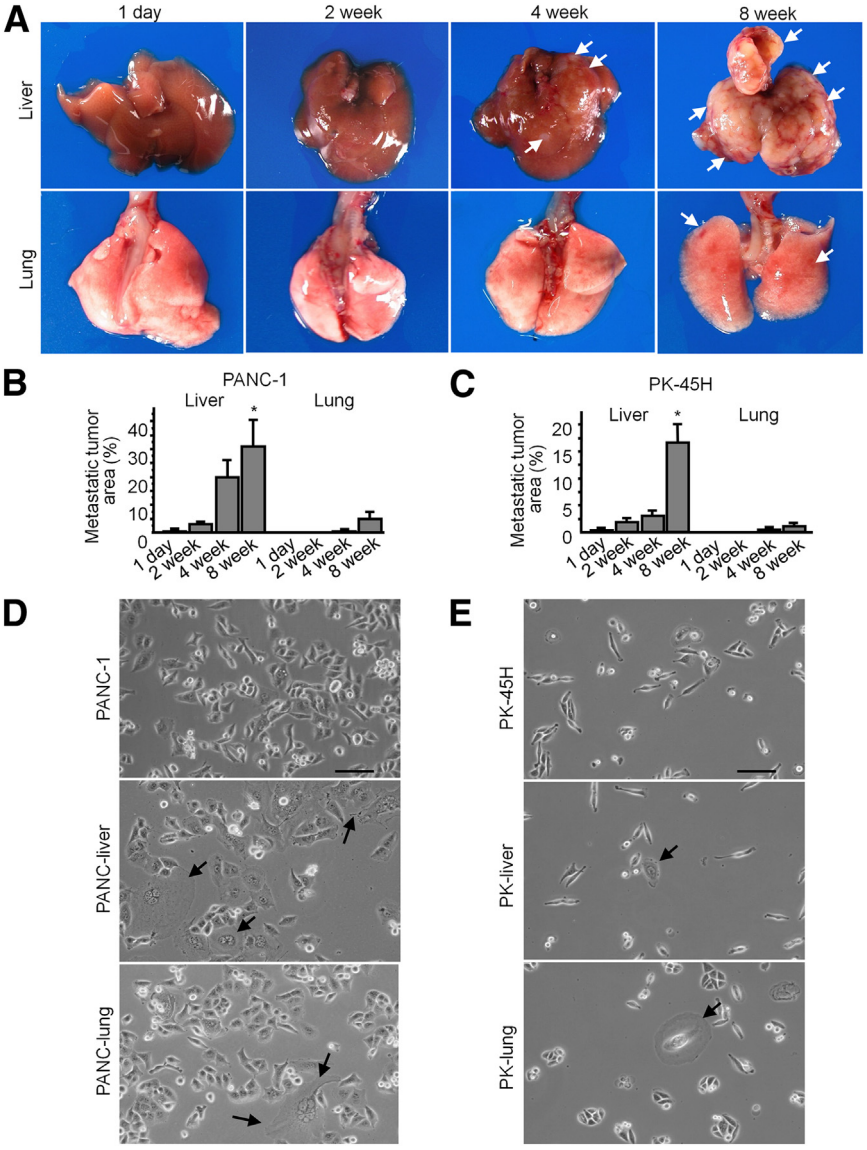

Figure 1 **A:** Macroscopic appearance of liver and lung after intrasplenic injection of PANC-1 human PDAC cells. **Arrows** indicate metastatic tumors. **B** and **C:** Metastatic tumor areas were calculated as a percentage of HLA^+ areas in liver and lung. **D** and **E:** Morphological changes in the cells derived from metastatic tumors of NOG mice (phase-contrast microscopy) included cells with large and polygonal morphology (**arrows**). Data are expressed as means ± SEM. $*P < 0.05$ versus other time points. Scale bar = 100 μm.

(Supplemental Figure S2A). Human mtDNA was detected in liver at 1 day and 2 weeks, and in liver and lung at 4 weeks. Moreover, at 8 weeks, human mtDNA was detected in liver, lung, heart, and kidney of NOG mice, but not in brain. Conversely, mouse-specific mtDNA was detected in all of the organs, but not in PANC-1 cells.

In contrast to our findings in NOG mice, at 24 hours after injection of PANC-1 cells into the spleen of nude mice, human-specific mtDNA was detected in the liver, but these cells did not yield macroscopically visible metastases in liver. Moreover, there were no visible metastases, and human-specific mtDNA was not detected by PCR in any of the above organs, all of which were analyzed at weekly intervals for 8 weeks (data not shown).

Isolation and Characterization of Human PDAC Cells Derived from Metastatic Tumors Arising in NOG Mice

To analyze the cell behavior of metastatic tumors, we harvested PANC-1 and PK-45H cells from liver and lung tumors of NOG mice at 8 weeks after xenotransplantation, when there was significant metastatic burden in both tissues in both cell lines (Figure 1, B and C). PANC-1 and PK-45H cells derived from liver tumors (PANC-liver and PK-liver) and from lung tumors (PANC-lung and PK-lung) expressed human-specific mitochondrial genes, but not mouse-specific mitochondrial genes (Supplemental Figure S2, B and C). Compared with parental PANC-1 or PK-45H cells, some of the cells derived from metastatic tumors of NOG mice (PANC-liver, PANC-

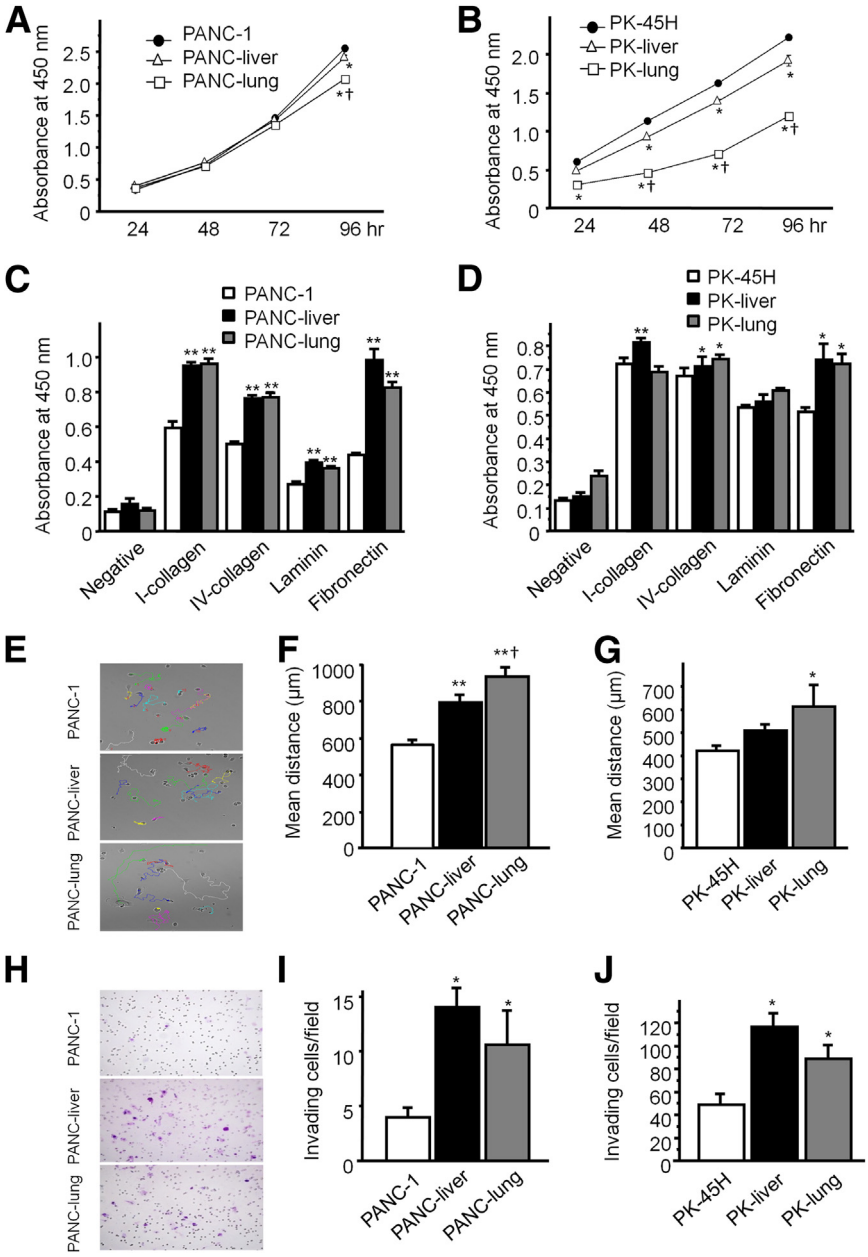

Figure 2 Cell growth, attachment, migration, and invasion assays of human PDAC cells derived from metastatic tumors of NOG mice. **A** and **B:** Cell growth of PANC-1 and PK-45H was analyzed by a WST-8 cell-counting assay. **C** and **D:** Attachment assay of cells to extracellular matrices. **E**–**G:** Single-cell movement was monitored by time-lapse microscopy. **H**–**J:** Cell invasion was analyzed by Boyden chamber assay. Data are expressed as means ± SEM. $*P < 0.05$, $**P < 0.01$ versus parental cells. $^{\dagger}P < 0.05$ versus liver cells. Original magnification, ×100 (**E**); ×200 (**H**).

lung, PK-liver, and PK-lung) were very large and exhibited a polygonal morphology (Figure 1, D and E).

Compared with parental cells, cells derived from pulmonary or hepatic metastatic lesions exhibited attenuated growth rates, especially in the case of PK-lung cells (Figure 2, A and B), but increased cell attachment to components of the extracellular matrix, including type I and IV collagen and fibronectin (Figure 2, C and D). PANC-liver and PANC-lung cells also exhibited increased attachment to laminin, whereas the attachment of PK-liver and PK-lung cells was not altered by laminin (Figure 2, C and D). By contrast, PANC-liver cells exhibited increased motility, compared with parental cells (Figure 2, E and F), and PANC-lung cells exhibited greater motility than PANC-liver cells (Figure 2, E and F). In the case of PK-45H cells, only PK-lung cells exhibited significantly increased motility, compared with parental cells (Figure 2G). Moreover, in Boyden chamber invasion assays, all four metastatic cell lines exhibited increased invasion, compared with the corresponding parental cells (Figure 2, H–J).

Tail-Vein Injection of Metastatic Cells

To assess the metastatic potential of cells derived from metastatic foci, we performed tail-vein injection of PANC-liver and PANC-lung cells in NOG mice. At 8 weeks after injection, PANC-liver and PANC-lung cells formed more macroscopically visible tumors in liver and lung, compared with parental PANC-1 cells (Figure 3, A and B). Some of the hepatic lesions were very large (Figure 3A), whereas the pulmonary lesions appeared as small red spots, indicative of small areas of hemorrhage (Figure 3B). Compared with parental cells, which formed metastases in only 50% of the cases, there were more HLA^+ areas in liver and lung after injection of PANC-liver and PANC-lung cells, and both organs exhibited metastatic lesions in 100% of cases (Figure 3, C and D, and Supplemental Table S2). There were no tumors and other significant changes in the brain.

To confirm these results, we performed studies using an orthotopic model. Compared with parental cells, PANC-liver cells formed larger metastatic lesions in both liver and lung, whereas PANC-lung cells formed larger metastatic lesions in lung (Figure 3E). Moreover, PK-liver and PK-lung cells formed larger metastatic lesions in liver and lung, respectively, compared with parental cells (Figure 3F).

PDAC Cells Derived from Metastatic Lesions Exhibit Features Suggestive of Cancer Stem Cells and EMT

In view of the potential role of CSC and EMT in metastasis, we next sought to determine whether our metastatic cells

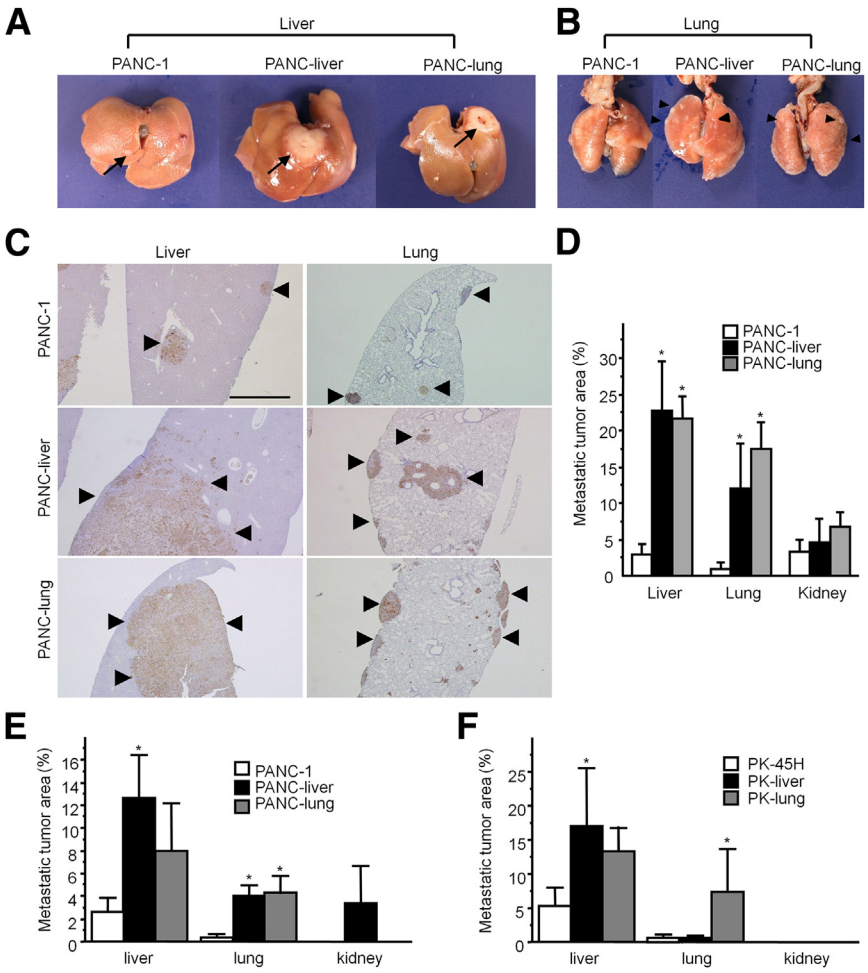

Figure 3 *In vivo* metastasis of human PDAC cells derived from metastatic tumors of NOG mice. **A** and **B:** Tumors of liver (**arrows**, **A**) and lung (**arrowheads**, **B**) after tail-vein injection of cells. **C:** HLA^+ metastatic tumor cells (**arrowheads**) in liver and lung. **D:** Metastatic tumor area, calculated as the HLA^+ area divided by the total area (liver, lung, or kidney) and then multiplied by 100. **E** and **F:** Metastatic tumor areas in liver, lung, or kidney after orthotopic implantation of the cells. Data are expressed as means ± SEM. $*P < 0.05$ versus PANC-1 cells. Scale bar = 100 μm.

exhibited features consistent with either CSC or EMT. Accordingly, we performed sphere-formation assays and side-population analysis with all four cell lines. Cells were plated in ultra-low attachment plates supplemented with EGF and FGF-2, and sphere formation was monitored (Figure 4A). PANC-liver, PANC-lung, PK-liver, and PK-lung cells formed a greater number of spheres, compared with their parental cells (Figure 4, B and C). Moreover, PANC-liver and PANC-lung cells exhibited increased side-population fraction, compared with parental cells (Figure 4, D and E). By contrast, in PK-45H cells no side-population cells were detected by flow cytometry.

Next, we examined expression of CSC markers. As determined by RT-qPCR, aldehyde dehydrogenase mRNA level was increased in PANC-liver, PANC-lung, PK-liver, and PK-lung cells, compared with the corresponding parental cells (Figure 4, F and G). Nestin mRNA level was increased in PANC-lung, PANC-liver, and PK-lung cells, but not in PK-liver cells, compared with the corresponding parental cells (Figure 4, H and I). Moreover, ABCG2 expression was increased in PANC-lung but not PANC-liver cells, and in both PK-liver and PK-lung cells (Figure 4, J and K). However, the expression of CD44, CD133, c-Met, and HGF (which also have been described as CSC markers) was similar in parental and metastatic cells (Supplemental Figure S3, A–G), except that CD133 mRNA was increased in PK-liver cells and HGF mRNA was not detectable in PK-45H cells. Flow cytometry analysis revealed higher nestin expression in metastatic cells, compared with parental cells (Supplemental Figure S4A). Furthermore, various levels of coexpression of nestin and other CSC markers were detected in metastatic PANC-1 and PK-45H cells (Supplemental Figure S4, B–G).

To confirm the increase of CSCs in metastatic lesions, we performed IHC analysis for CSC markers and for the cell proliferation marker Ki-67 at 8 weeks after xenotransplantation. Metastatic tumor cells in liver exhibited various levels of immunoreactivity for ALDH1A1 and nestin in the cytoplasm and on the cell membrane, for ABCG2 and CD44 on the cell membrane, and for Ki-67 in the nucleus (Figure 5A).

Next, we analyzed the percentage of CSC marker–positive cells in NOG mice in each organ at each time point (Figure 5, B–F). At 8 weeks after xenotransplantation, the percentage of nestin$^+$ cells was increased in lung, compared with pancreas and liver (Figure 5C). In liver, the percentage

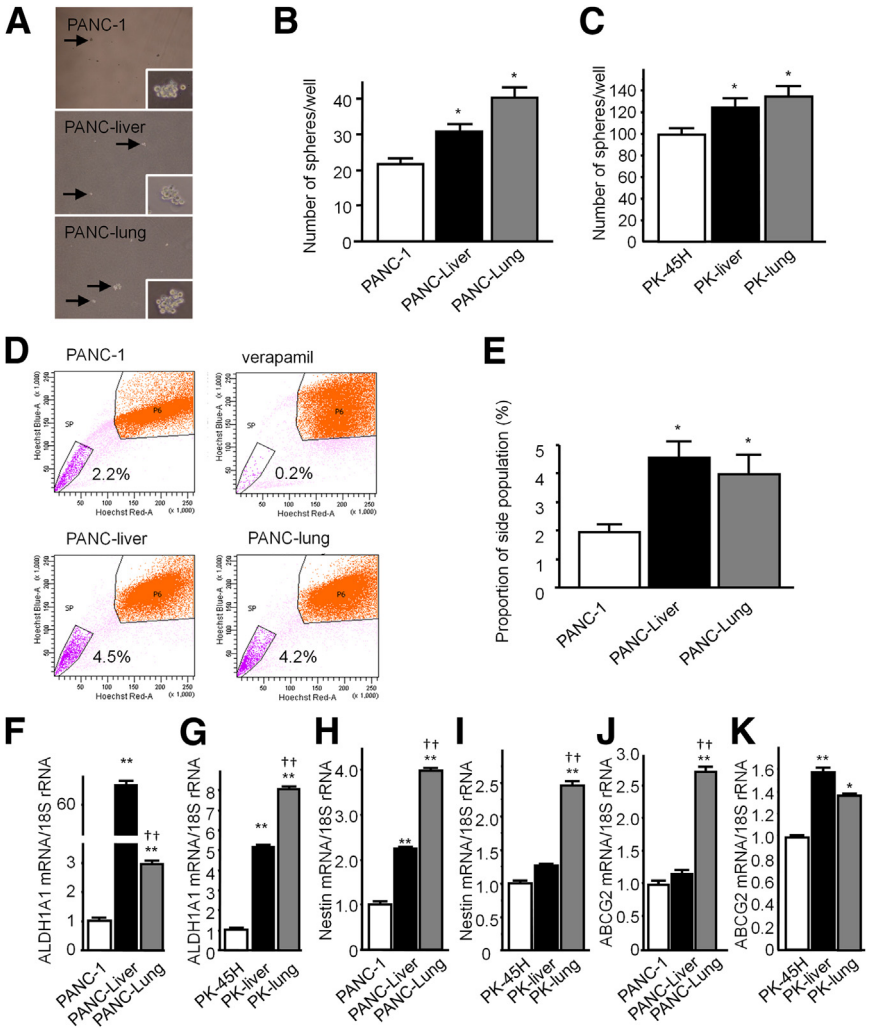

Figure 4 Stemness of human PDAC cells derived from metastatic tumors of NOG mice. **A:** Sphere-forming assay of cells. Spheres (**arrows**) are shown at higher magnification in the **insets**. **B** and **C:** Number of spheres per well for PANC-1 and PK-45H cells. **D** and **E:** Proportion of side-population fraction (pink) and major population (orange), as determined by flow cytometry (**D**) and quantification (**E**). **F–K:** Expression of the CSC markers ALDH1A1 (**F** and **G**), nestin (**H** and **I**), and ABCG2 (**J** and **K**). $*P < 0.05$, $**P < 0.01$ versus parental cells. $^{\dagger\dagger}P < 0.01$ versus metastatic cells from liver. Original magnification: ×40 (**main images**); ×100 (**insets**).

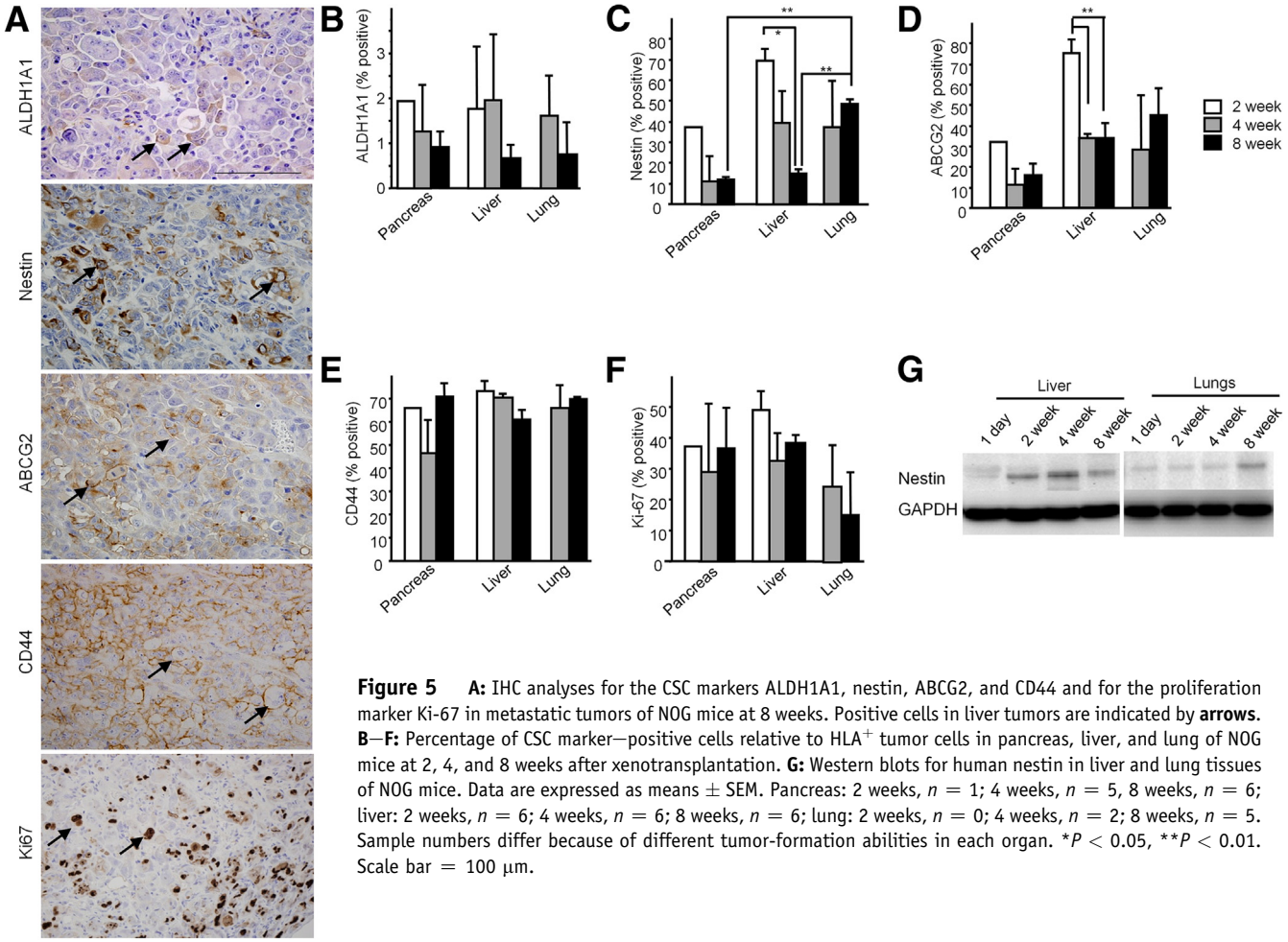

Figure 5 **A:** IHC analyses for the CSC markers ALDH1A1, nestin, ABCG2, and CD44 and for the proliferation marker Ki-67 in metastatic tumors of NOG mice at 8 weeks. Positive cells in liver tumors are indicated by **arrows**. **B**—**F:** Percentage of CSC marker—positive cells relative to HLA^+ tumor cells in pancreas, liver, and lung of NOG mice at 2, 4, and 8 weeks after xenotransplantation. **G:** Western blots for human nestin in liver and lung tissues of NOG mice. Data are expressed as means ± SEM. Pancreas: 2 weeks, $n = 1$; 4 weeks, $n = 5$, 8 weeks, $n = 6$; liver: 2 weeks, $n = 6$; 4 weeks, $n = 6$; 8 weeks, $n = 6$; lung: 2 weeks, $n = 0$; 4 weeks, $n = 2$; 8 weeks, $n = 5$. Sample numbers differ because of different tumor-formation abilities in each organ. $^*P < 0.05$, $^{**}P < 0.01$. Scale bar = 100 μm.

of $nestin^+$ cells was decreased at 8 weeks, compared with 2 weeks (Figure 5C), and this decrease was confirmed by immunoblotting (Figure 5G). Similarly, the percentage of $ABCG2^+$ cells was decreased in liver at 4 and 8 weeks, compared with 2 weeks (Figure 5D). By contrast, the percentage of $ALDH1A1^+$, $CD44^+$, and $Ki\text{-}67^+$ cells was similar in pancreas, liver, and lung (Figure 5, B, E and F), whereas no CD133 immunoreactivity was detected in all specimens. Thus, nestin and ABCG2 levels were increased in metastatic cells, and remained elevated in lung metastases, but decreased over time in liver metastases.

EMT Markers in PDAC Cells Derived from Metastatic Tumors

To assess the role of EMT in the metastatic process, we next examined expression of EMT markers. E-cadherin mRNA levels in all four metastatic cell lines were lower than in the corresponding parental cells, and were lowest in PANC-lung and PK-lung cells (Figure 6, A and B). By contrast, vimentin mRNA levels were generally similar in metastatic and parental cells (Figure 6, C and D), except that PK-liver cells expressed higher levels of vimentin, compared with parental and PK-lung cells (Figure 6D). Moreover, at 8 weeks after splenic injection, hepatic metastases exhibited relatively low-intensity E-cadherin immunoreactivity on the cell membrane (Figure 6E) and strong vimentin immunoreactivity in the cytoplasm (Figure 6F), whereas the percentage of $E\text{-cadherin}^+$ cells relative to HLA^+ tumor cells decreased in lung, compared with pancreas and liver (Figure 6G). By contrast, strong vimentin immunoreactivity persisted at 8 weeks in all three organs (Figure 6H).

Expression of CSC and EMT Markers in Human PDAC Autopsy Cases

We next sought to compare the immunostaining of CSC and EMT markers in primary and metastatic lesions in 12 autopsy cases of PDAC patients. Each CSC or EMT marker was expressed in the different types of cells at various levels in human nontumorous pancreatic tissues (Supplemental Figure S5). CD44, CD133, and E-cadherin were expressed in ductal cells; CD44 and E-cadherin were expressed in acinar cells; vimentin was expressed in mesenchymal cells; and nestin was not expressed. In addition to hepatic metastases, we examined other metastatic lesions (lymph node,

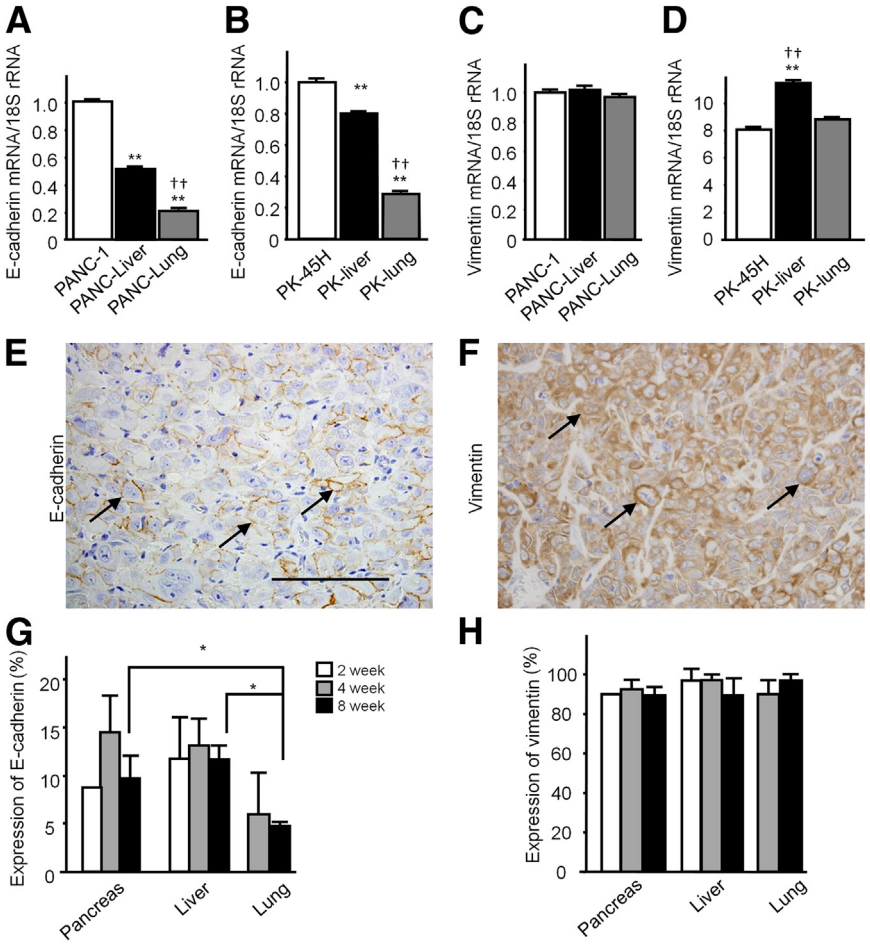

Figure 6 **A**—**D:** Expression of the EMT markers E-cadherin and vimentin in cells derived from metastatic foci of NOG mice. **E** and **F:** IHC analysis for E-cadherin and vimentin in metastatic liver tumors of NOG mice at 8 weeks. Positive cells are indicated by **arrows**. **G** and **H:** Percentage of EMT marker—positive cells relative to HLA^+ tumor cells in liver and lung of NOG mice. $^*P < 0.05$ versus lung cells. $^{**}P < 0.01$ versus parental cells. $^{\dagger\dagger}P < 0.01$ versus metastatic cells from liver. Scale bar = 100 μm.

lung, and omentum). Immunoreactivity of nestin and ABCG2 was increased in metastatic lesions, compared with primary lesions, whereas E-cadherin immunostaining was decreased (Supplemental Figure S6A). The percentage of $nestin^+$ cells was not significantly increased in liver lesions, but was significantly increased in other metastatic lesions (Supplemental Figure S6C). By contrast, ABCG2 immunoreactivity was significantly increased (Supplemental Figure S6D), and E-cadherin immunoreactivity was significantly decreased, in all tested metastases (Supplemental Figure S6G). However, ALDH1A1, CD44, CD133, and vimentin immunoreactivity did not differ significantly between the metastatic lesions and the primary PDAC tumor (Supplemental Figure S6, B, E, F, and H).

Effects of Nestin Silencing on Sphere Formation and Metastasis

In view of the increased expression of nestin in metastasis-derived cell lines and in both mouse and human metastatic lesions, we next assessed the consequences of nestin knockdown on sphere formation and metastasis. shRNAs targeting nestin were stably transfected into PANC-lung cells, and nestin mRNA and protein levels were assessed in scrambled sequence subcloned sham vector stably transfected cells (Sc-1 and Sc-10) and in nestin shRNA stably transfected cells (Sh-1 and Sh-2), using RT-qPCR and immunoblotting (Figure 7, A and B). Selected clones were then tested for their ability to form spheres. Nestin shRNA—transfected cells exhibited decreased sphere formation, compared with parental and Sc cells (Supplemental Figure S7, A and B), and decreased slug mRNA expression (Supplemental Figure S7C). By contrast, expression of snail, zeb1, and zeb2 mRNA was not altered (Supplemental Figure S7, D—F), and twist mRNA was not detected in these cells (data not shown). PANC-1 exhibited high nestin expression levels, but KLM-1 and PK-8 exhibited no or low nestin expression levels. These observations suggest that nestin may regulate EMT by modulating slug expression.

Next, the same cells were injected into the spleen of NOG mice ($n = 4$ per cell line). At 6 weeks after injection, some mice exhibited weight loss (approximately 10%), and therefore the experiment was terminated at that time point. PANC-lung cells exhibited more aggressive metastatic tumors in liver (Figure 7C), compared with parental PANC-1 cells (Figure 1A). However, PANC-lung cells transfected with shRNA targeting nestin (Sh-1 and Sh-2) exhibited a dramatic decrease in liver metastasis, compared with parental

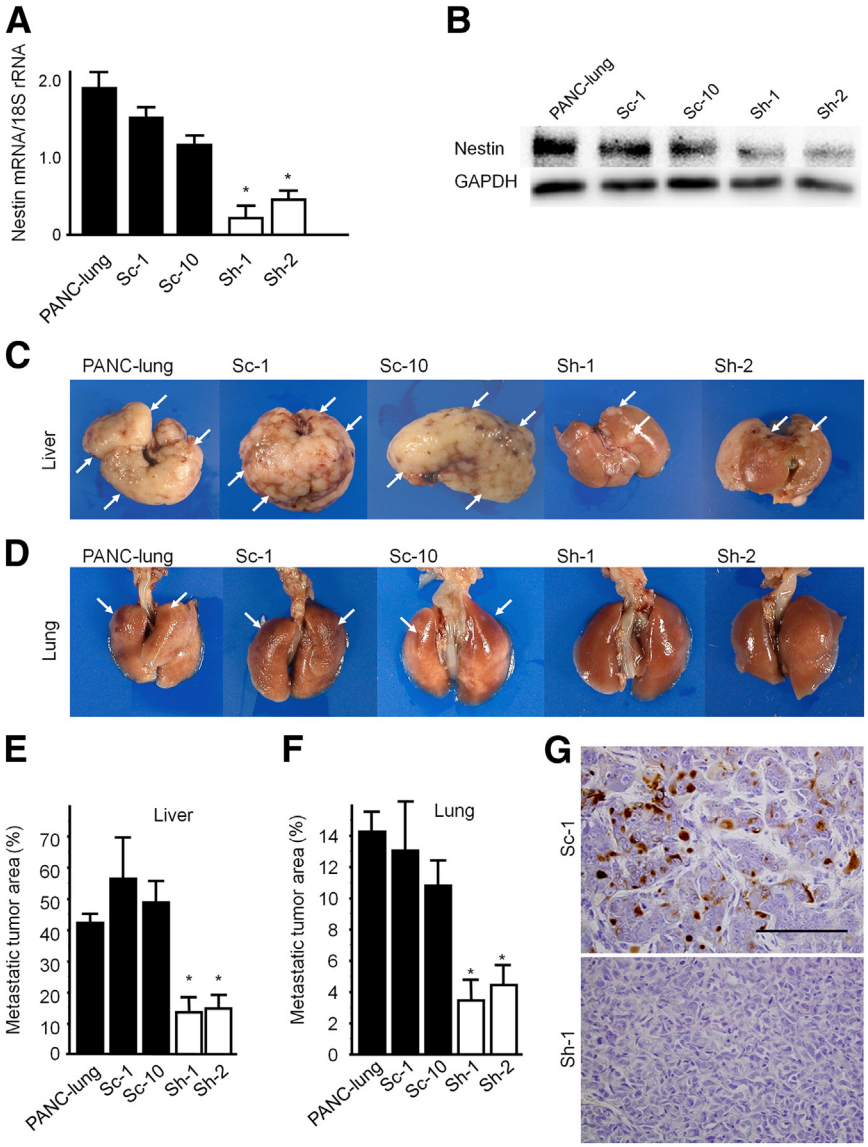

Figure 7 Inhibition of metastasis using shRNA targeting nestin of PANC lung cells. Stable transfection of shRNA targeting nestin into PANC lung cells. **A:** RT-qPCR analysis of nestin in shRNA-transfected clones. **B:** Western blots for nestin confirm decreased expression in shRNA-transfected clones. **C** and **D:** Stable transfection of shRNA targeting nestin suppressed liver and lung metastases of NOG mice. **Arrows** indicate metastatic tumors (in the liver, **C**) or hemorrhage (in the lung, **D**). **E** and **F:** Metastatic tumor areas in liver and lung in shRNA-transfected clones. **G:** IHC analysis of nestin in hepatic metastases. Scale bar = 100 μm. *$P < 0.05$ versus parental and sham cells. Sc, sham transfection; Sh, shRNA transfection.

PANC-lung cells and the sham-transfected clones (Sc-1 and Sc-10) (Figure 7C). PANC-lung and sham-transfected clones exhibited nondescript red nodules in lung, indicative of hemorrhage or congestion due to the presence of pulmonary metastases (Figure 7D). Moreover, the percentage of HLA$^+$ area in liver and lung was significantly decreased in Sh-1 and Sh-2 lesions, compared with the lesions caused by the corresponding control cells (Figure 7, E and F). IHC analysis of nestin in liver confirmed decreased nestin expression in shRNA-transfected clones (Figure 7G). Thus, increased nestin expression in metastatic cells plays important roles in tumor metastasis, and inhibition of nestin expression in pancreatic cancer cells could suppress metastasis.

Next, we determined the effects of nestin shRNA in KLM-1 and PK-8 cells, which express low or very low nestin levels (Supplemental Figure S7G). In these cells, nestin shRNA did not alter cell migration or sphere formation (Supplemental Figure S7, H and I). Thus, the effects of nestin shRNA were not due to nonspecific effects on pancreatic cancer cells.

Analyses of Inflammatory Cells in PDAC Tissue

The failure of nude mice (which are not as severely immunodeficient as NOG mice) to develop metastases after intrasplenic injection of human PDAC cells raised the possibility that the immune system could be activated to suppress metastatic disease. To examine this possibility, IHC analysis was performed to detect macrophages (CD68 for human and MAC-2 for mouse), T cells (CD3), B cells (CD20), and dendritic cells (CD11c) in human hepatic metastases, in metastatic lesions in NOG mice after intrasplenic injection of PDAC cells, and in nude mice after orthotopic injection of these cells (Supplemental Figure S8). Hepatic metastases in human PDAC and in an orthotopic model in nude mice exhibited marked infiltration of the metastatic lesions by macrophages and slight infiltration with T cells and B cells. By contrast, there were only a few MAC-2$^+$ macrophages in the hepatic metastases in NOG mice, and no natural killer cells

were detected in liver tissues from nude and NOG mice (data not shown).

Discussion

The intrasplenic model of PDAC consists of the injection of cancer cells into the spleen and removal of the spleen 1 minute later, which allows sufficient time for the cancer cells to flow from the spleen into the splenic vein, and then into the portal vein and liver.[15] Although this is not a frequently used model, it can provide important information on the metastatic process. In the present study, at 1 day after intrasplenic injection of human PDAC cells, HLA^+ PDAC cells were detected in liver of nude and NOG mice, but not in other organs, suggesting that the cancer cells may be trapped in the liver immediately after injection and only later disseminate to other organs. In the NOG mice, sites of metastasis included lung and kidney, which are known sites for PDAC metastasis, as well as the heart, which is a less frequent metastatic site.[16] Metastases to pancreas were also observed in these mice, underscoring the observation that PDAC may also form intrapancreatic metastases,[17] and that certain cancers (eg, lung, kidney, and breast cancers) may metastasize to normal pancreas.[18]

Surprisingly, nude mice did not develop metastases after intrasplenic injection of human PDAC cells, even though they readily formed metastases after intrapancreatic injection. Moreover, metastatic lesions in human PDAC and in an orthotopic nude mouse model contained many infiltrating macrophages, whereas the metastatic lesions in NOG mice harbored only a paucity of infiltrating macrophages. Taken together, these observations raise the possibility that the immune system could be activated in PDAC patients to suppress metastatic disease.

Human PDAC cells derived from metastatic liver and lung tumors of NOG mice uniformly formed metastatic foci after tail-vein injection and exhibited increased sphere formation and side-population fraction, attenuated proliferation, and increased expression of the CSC markers ALDH1A1, nestin, and ABCG2. Nestin and ABCG2 levels were especially elevated in lung metastases, and nearly all tested metastatic lesions in PDAC patients exhibited increased ABCG2 and nestin expression. Moreover, the CSC fraction was high in early hepatic metastases, but decreased with time. Taken together, these findings indicate that the cancer cells isolated from metastatic lesions in NOG mice have many of the features associated with CSCs, and suggest that metastatic CSCs can convert to nonstem cancer cells, which is in agreement with recent concepts regarding active CSC plasticity whereby nonstem cancer cells can acquire CSC features and CSCs can lose their stem cell characteristics.[19] It is also possible that $nestin^+$ cells metastasize out of the liver, explaining both their decreased prevalence with time in liver lesions and their abundance in distant metastases.

Nestin is a class VI intermediate filament protein that requires other intermediate filament proteins to form filamentous structures.[20] Nestin is also a stem-cell marker, and activation of oncogenic K-ras in the nestin cell lineage in the pancreas leads to pancreatic intraepithelial neoplasia that progresses to PDAC after an acute inflammatory insult.[21] Moreover, we have previously reported that nestin contributes to pancreatic cancer cell migration, invasion, and metastasis via alterations in E-cadherin and F-actin, and that restoring nestin expression in shRNA-transfected PANC-1 and PK-45H cells leads to enhanced invasive behavior.[9] In the present study, we demonstrated that expression levels of slug, a major EMT-associated transcription factor, was regulated by nestin in PANC-1 cells. We also determined that highly metastatic pancreatic cancer cells express nestin in both mouse and human metastatic lesions, and that nestin expression correlates with EMT and CSC features. Moreover, suppression of nestin expression was associated with a marked decrease in sphere formation *in vitro* and metastatic potential *in vivo*. Taken together, our findings confirm that nestin is a CSC marker in PDAC, and suggest that targeting nestin could help suppress CSCs and metastasis in PDAC. Inasmuch as pancreatic CSCs contribute to PDAC growth and chemoresistance, and their resistance can be partially overcome by targeting the pathways that promote CSCs,[22–24] our findings also suggest that targeting nestin could be an important component of various combinational therapeutic strategies in PDAC.

Cell attachment to the extracellular matrix was increased in metastasis-derived pancreatic cancer cells, but these cells exhibited enhanced motility (especially the cancer cells derived from lung metastases). Invasion through Matrigel was also increased in the metastatic cancer cells, and both increased migration and invasion were associated with features consistent with EMT, as evidenced by decreased E-cadherin mRNA and protein levels and by the large, polygonal features of these cells. These findings suggest that cancer cell heterogeneity may correlate with the presence of CSCs, which help to promote distant metastases.[25,26] Given that EMT and stemness have a close causal relationship,[27] our findings further underscore the potential benefit of targeting nestin to increase therapeutic effectiveness in PDAC.

Acknowledgments

We thank Dr. Masahito Hagio for helpful discussion and Kiyoko Kawahara, Taeko Suzuki, Yuji Yanagisawa, and Yoko Kawamoto (Nippon Medical School, Tokyo, Japan) for excellent technical assistance.

Supplemental Data

Supplemental material for this article can be found at *http://dx.doi.org/10.1016/j.ajpath.2013.11.014*.

References

1. Jemal A, Siegel R, Ward E, Hao Y, Xu J, Murray T, Thun MJ: Cancer statistics, 2008. CA Cancer J Clin 2008, 58:71–96

2. Bidard FC, Pierga JY, Vincent-Salomon A, Poupon MF: A "class action" against the microenvironment: do cancer cells cooperate in metastasis? Cancer Metastasis Rev 2008, 27:5−10
3. Suemizu H, Monnai M, Ohnishi Y, Ito M, Tamaoki N, Nakamura M: Identification of a key molecular regulator of liver metastasis in human pancreatic carcinoma using a novel quantitative model of metastasis in NOD/SCID/gammacnull (NOG) mice. Int J Oncol 2007, 31:741−751
4. Nakamura M, Suemizu H: Novel metastasis models of human cancer in NOG mice. Curr Top Microbiol Immunol 2008, 324:167−177
5. Bissell MJ, Labarge MA: Context, tissue plasticity, and cancer: are tumor stem cells also regulated by the microenvironment? Cancer Cell 2005, 7:17−23
6. Hermann PC, Huber SL, Herrler T, Aicher A, Ellwart JW, Guba M, Bruns CJ, Heeschen C: Distinct populations of cancer stem cells determine tumor growth and metastatic activity in human pancreatic cancer. Cell Stem Cell 2007, 1:313−323
7. Seton-Rogers S: Metastasis: dynamic interactions. Nat Rev Cancer 2012, 12:378−379
8. Charafe-Jauffret E, Ginestier C, Iovino F, Tarpin C, Diebel M, Esterni B, Houvenaeghel G, Extra JM, Bertucci F, Jacquemier J, Xerri L, Dontu G, Stassi G, Xiao Y, Barsky SH, Birnbaum D, Viens P, Wicha MS: Aldehyde dehydrogenase 1-positive cancer stem cells mediate metastasis and poor clinical outcome in inflammatory breast cancer. Clin Cancer Res 2010, 16:45−55
9. Matsuda Y, Naito Z, Kawahara K, Nakazawa N, Korc M, Ishiwata T: Nestin is a novel target for suppressing pancreatic cancer cell migration, invasion and metastasis. Cancer Biol Ther 2011, 11:512−523
10. Wellner U, Schubert J, Burk UC, Schmalhofer O, Zhu F, Sonntag A, Waldvogel B, Vannier C, Darling D, zur Hausen A, Brunton VG, Morton J, Sansom O, Schüler J, Stemmler MP, Herzberger C, Hopt U, Keck T, Brabletz S, Brabletz T: The EMT-activator ZEB1 promotes tumorigenicity by repressing stemness-inhibiting microRNAs. Nat Cell Biol 2009, 11:1487−1495
11. Brabletz T, Jung A, Spaderna S, Hlubek F, Kirchner T: Opinion: migrating cancer stem cells−an integrated concept of malignant tumour progression. Nat Rev Cancer 2005, 5:744−749
12. Ono K, Satoh M, Yoshida T, Ozawa Y, Kohara A, Takeuchi M, Mizusawa H, Sawada H: Species identification of animal cells by nested PCR targeted to mitochondrial DNA. In Vitro Cell Dev Biol Anim 2007, 43:168−175
13. Ishiwata T, Matsuda Y, Yamamoto T, Uchida E, Korc M, Naito Z: Enhanced expression of fibroblast growth factor receptor 2 IIIc promotes human pancreatic cancer cell proliferation. Am J Pathol 2012, 180:1928−1941
14. Ishiwata T, Teduka K, Yamamoto T, Kawahara K, Matsuda Y, Naito Z: Neuroepithelial stem cell marker nestin regulates the migration, invasion and growth of human gliomas. Oncol Rep 2011, 26: 91−99
15. Murakami M, Nagai E, Mizumoto K, Saimura M, Ohuchida K, Inadome N, Matsumoto K, Nakamura T, Maemondo M, Nukiwa T, Tanaka M: Suppression of metastasis of human pancreatic cancer to the liver by transportal injection of recombinant adenoviral NK4 in nude mice. Int J Cancer 2005, 117:160−165
16. Merkle EM, Boaz T, Kolokythas O, Haaga JR, Lewin JS, Brambs HJ: Metastases to the pancreas. Br J Radiol 1998, 71:1208−1214
17. Ogawa M, Kawaguchi Y, Uchida T, Ito H, Mine T: A case of small pancreatic cancer with intra-pancreatic metastasis diagnosed by endoscopic ultrasound. Tokai J Exp Clin Med 2011, 36:75−78
18. Chiles C, Woodard PK, Gutierrez FR, Link KM: Metastatic involvement of the heart and pericardium: CT and MR imaging. Radiographics 2001, 21:439−449
19. Chaffer CL, Brueckmann I, Scheel C, Kaestli AJ, Wiggins PA, Rodrigues LO, Brooks M, Reinhardt F, Su Y, Polyak K, Arendt LM, Kuperwasser C, Bierie B, Weinberg RA: Normal and neoplastic nonstem cells can spontaneously convert to a stem-like state. Proc Natl Acad Sci USA 2011, 108:7950−7955
20. Steinert PM, Chou YH, Prahlad V, Parry DA, Marekov LN, Wu KC, Jang SI, Goldman RD: A high molecular weight intermediate filament-associated protein in BHK-21 cells is nestin, a type VI intermediate filament protein. Limited co-assembly in vitro to form heteropolymers with type III vimentin and type IV alpha-internexin. J Biol Chem 1999, 274:9881−9890
21. Carrière C, Young AL, Gunn JR, Longnecker DS, Korc M: Acute pancreatitis accelerates initiation and progression to pancreatic cancer in mice expressing oncogenic Kras in the nestin cell lineage. PLoS One 2011, 6:e27725
22. Rajeshkumar NV, Rasheed ZA, García-García E, López-Ríos F, Fujiwara K, Matsui WH, Hidalgo M: A combination of DR5 agonistic monoclonal antibody with gemcitabine targets pancreatic cancer stem cells and results in long-term disease control in human pancreatic cancer model. Mol Cancer Ther 2010, 9:2582−2592
23. Lonardo E, Hermann PC, Mueller MT, Huber S, Balic A, Miranda-Lorenzo I, Zagorac S, Alcala S, Rodriguez-Arabaolaza I, Ramirez JC, Torres-Ruíz R, Garcia E, Hidalgo M, Cebrián DÁ, Heuchel R, Löhr M, Berger F, Bartenstein P, Aicher A, Heeschen C: Nodal/Activin signaling drives self-renewal and tumorigenicity of pancreatic cancer stem cells and provides a target for combined drug therapy. Cell Stem Cell 2011, 9:433−446
24. Bednar F, Simeone DM: Pancreatic cancer stem cell biology and its therapeutic implications. J Gastroenterol 2011, 46:1345−1352
25. Yachida S, Jones S, Bozic I, Antal T, Leary R, Fu B, Kamiyama M, Hruban RH, Eshleman JR, Nowak MA, Velculescu VE, Kinzler KW, Vogelstein B, Iacobuzio-Donahue CA: Distant metastasis occurs late during the genetic evolution of pancreatic cancer. Nature 2010, 467:1114−1117
26. Campbell PJ, Yachida S, Mudie LJ, Stephens PJ, Pleasance ED, Stebbings LA, Morsberger LA, Latimer C, McLaren S, Lin ML, McBride DJ, Varela I, Nik-Zainal SA, Leroy C, Jia M, Menzies A, Butler AP, Teague JW, Griffin CA, Burton J, Swerdlow H, Quail MA, Stratton MR, Iacobuzio-Donahue C, Futreal PA: The patterns and dynamics of genomic instability in metastatic pancreatic cancer. Nature 2010, 467:1109−1113
27. Li J, Zhou BP: Activation of β-catenin and Akt pathways by Twist are critical for the maintenance of EMT associated cancer stem cell-like characters. BMC Cancer 2011, 11:49